

Novel fluorinated piperazine based-amino acid derivatives as antiplasmodial agents: Synthesis, bioactivity and computational studies

Charu Upadhyay¹, Shreya Bhattacharya², Sumit Kumar¹, Dharmender Kumar¹, Neha Bhadula¹, Brijesh Rathi^{3,4*}, Agam Prasad Singh^{2*}, Poonam^{1,4*}

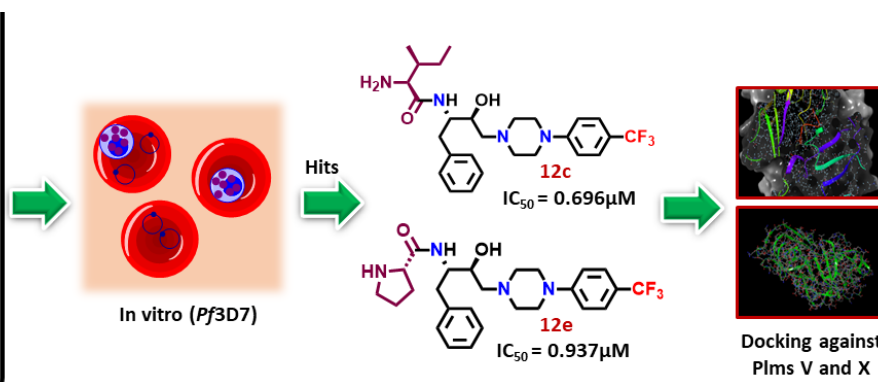
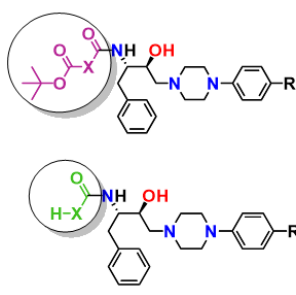
¹Department of Chemistry, Miranda House, University of Delhi, Delhi-110007, India. ²Infectious Diseases Laboratory, National Institute of Immunology, New Delhi 110067, India. ³Laboratory for Translational Chemistry and Drug Discovery, Department of Chemistry, Hansraj College, University of Delhi, Delhi, 110007, India. ⁴Delhi School of Public Health, Institute of Eminence, University of Delhi, Delhi, 110007, India.

Submitted on: 12-Jan-2023 Accepted and Published on: 20-Mar-2023

Article

ABSTRACT

Fluorinated Piperazine based amino acid derivatives



A library of twenty novel analogues of fluorinated, N-(3-hydroxy-1-phenyl-4-(4-phenylpiperazin-1-yl)alkyl)amides containing different amino acids were synthesized and tested for the activity against *Plasmodium falciparum* (Pf3D7) culture. All the tested compounds showed TC₅₀ values >100 μM on HepG2 cells. Hit analogues **12c** and **12e**, displayed IC₅₀ values in the sub-micromolar range, *i.e.*, 0.696±0.0462 μM and 0.937±0.0461 μM, respectively. Compounds **12c** and **12e** were also evaluated in combination with artemisinin, which slightly improved the activity of both the compounds with IC₅₀ values of 0.19 μM and 0.26 μM, respectively. For compounds **12c** and **12e**, *in-silico* studies were carried out. Overall, results obtained from both *in vitro* and *in-silico* studies, indicated that **12c** and **12e** were hit compounds with maximum potency.

Keywords: *Plasmodium falciparum*, heteroaromatic amino acid, antimalarial agent, in-vitro studies, in-silico studies

INTRODUCTION

Every year, millions of people worldwide suffer from malaria, a fatal disease caused by an infection with the protozoan parasite, *Plasmodium*.¹ In terms of its effects on public health and the economy, malaria continues to be a serious issue. In Africa, malaria was responsible for 93% of the estimated 435,000 deaths globally. Furthermore, *Plasmodium falciparum* (Pf) infections in youngsters are responsible for most of these fatalities. At least \$12 billion is lost to malaria in Africa each year.²

The parasite goes through two major stages in its life cycle: the liver stage and the blood stage. The blood stage of malaria is

responsible for most of the clinical manifestations of the disease, while the liver stage is typically asymptomatic. However, drugs that target the liver stage of the parasite (such as primaquine) are important for preventing relapses of the disease, while drugs that target the blood stage (such as chloroquine) are used for treating acute infections.³ Apart from these asexual stages, the sexual stage of the malaria parasite is also critical for the transmission of the disease between human hosts, as it allows the parasite to complete its life cycle inside the mosquito vector. The sexual stage of the malaria parasite, also known as the "gametocyte" stage, occurs in the human bloodstream after the parasite has undergone several rounds of replication in the red blood cells. During this stage, some of the parasite's daughter cells differentiate into either male (microgametocytes) or female (macrogametocytes) gametocytes.^{4,5}

A significant advancement in antimalarial therapy involves the usage of artesunate for the treatment of severe malaria and artemisinin combination therapies (ACTs) for uncomplicated

*Corresponding Author: Brijesh Rathi, Agam Prasad Singh, Poonam
Email: brijeshrathi@hrc.du.ac.in (BR), singhap@nii.ac.in (APS),
poonam.chemistry@mirandahouse.ac.in (P)



malaria.^{6,7} These medications have lowered mortality, accelerated recovery, and decreased treatment failure rates and infection transmission.⁸ Artemisinin (ART) derivatives are still effective in preventing *Pf* malaria in most malaria endemic regions, however emerging resistance in Southeast Asia's Greater Mekong subregion, is a serious concern.⁹

Unfortunately, antimalarial drug resistance is unavoidable and it develops gradually for around twenty years at which point it suddenly becomes prevalent.^{10,11} Despite significant progress in recent years, the development of an effective vaccine against malaria has proven challenging, hindering efforts to eradicate the disease. Therefore, designing novel antimalarial molecules must be a part of campaigns to combat the disease *i.e.*, intervene in parasite transmission and reduce fatality rates.

Amino acids play a vital role in the pharmaceutical industry. As a crucial synthetic precursor for drugs, biomaterials, biosensors, and drug delivery devices, amino acids are significant in the modern health industry. Coupling reactions between amino acids and heteroaromatic compounds lead to bioactive products.¹² Piperazine is well known heterocyclic moiety that enhances the potency of antimalarial scaffolds. For example, MMV253, UCT943 and KAF156 are antimalarial drugs containing piperazine moiety which are in the second phase of clinical trials. Moreover, the incorporation of -F/-CF₃ groups to such analogs showed better activity against different strains of malaria parasite.¹³ Hence, the introduction of piperazine and -F/-CF₃ groups containing different amino acids could be a rational design of molecules against malaria. In view of these observations, we have synthesized a library of twenty novel analogues of fluorinated, N-(3-hydroxy-1-phenyl-4-(4-phenylpiperazin-1-yl)alkyl)amides containing different amino acids (Figure 1). Further, all the synthesized analogs were tested for their *in-vitro* biological assays against the malaria parasite.

MATERIALS AND METHOD

Chemistry

The chemicals and solvents were all purchased from either GLR, TCI, or Sigma Aldrich in Canada; none were further refined before usage. Using 60 F₂₅₄ silica gel plates from Sigma-Merck, thin-layer chromatography (TLC) was examined to monitor and confirm the purity of the produced compounds. Microwave reactions were performed in microwave specific vial at 70 °C utilizing-controlled temperature with a 5-minute ramp and holding for 15 minutes with a 300 W power supply using the "Start Synth Microwave Synthesis Labstation" microwave apparatus. The solvent for the NMR spectroscopy investigation use was CDCl₃, with tetramethyl silane serving as an internal standard.

General synthetic procedure

Hydroxyethylamine (HEA) analogues **4** and **5** were synthesized using fluorinated piperazine **2** and **3**, respectively, following the previously described methods¹⁴. In a microwave tube, fluorinated piperazine **2-3**, (0.019 mol) and *tert*-butyl ((S)-1-((R)-oxiran-2-yl)-2-phenylethyl)carbamate **1** (0.019 mol) were dissolved in 5 mL ethanol and the contents were microwave irradiated at 300W, 70°C to yield corresponding Boc-protected HEA intermediates, **4-5**.¹⁵ The reaction was monitored by TLC. After the completion of the reaction, the solvent was extracted under reduced pressure using a rota-evaporator to give Boc-protected intermediates (**4-5**) as white solid. Then, compounds, **4** or **5** were mixed with 20% trifluoroacetic acid (TFA) in dichloromethane (DCM) at 0°C for an hour, resulting in deprotected HEA. The crude product was extracted using ethyl acetate and 1 M NaOH solution. Over sodium sulfate, the organic ethyl acetate layer was dried and filtered. The excess solvent was evaporated using a rota-evaporator to afford the required products **6** or **7**, respectively.

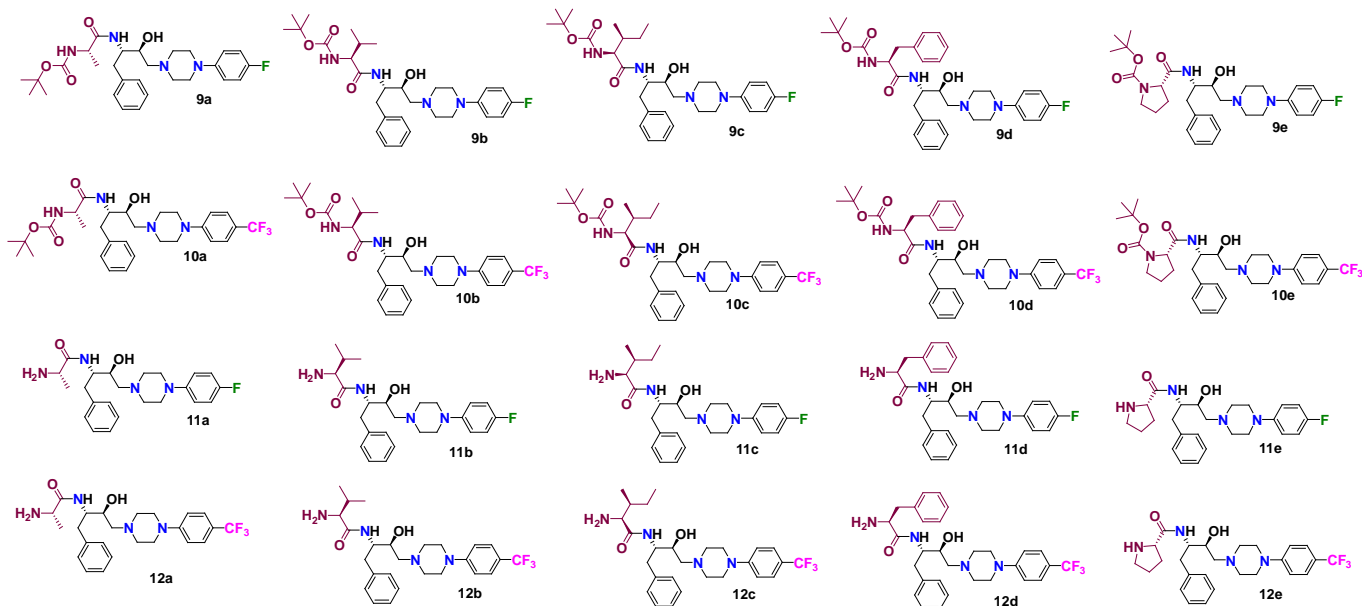


Figure 1. Chemical structures of all the novel synthesized fluorinated piperazine based-amino acid derivatives.

In a round bottom (RB) flask, Boc-protected amino acids (**8a-8e**) were dissolved in DCM and triethyl amine (TEA) (3 eq, 5.82 mol) was added to it dropwise. After 20 minutes, EDC•HCl (3 eq, 5.82 mol) was added to the same RB flask, followed by the addition of HOBt (3 eq, 5.82 mol) after another 20 minutes. The reaction was stirred for 30 minutes. Later, compound (**6-7**) was added to the same RB flask. All these above-mentioned additions were performed at 0 °C and then the reaction mixture was allowed to stir for 24 hours at room temperature. After the completion of the reaction, monitored by TLC, the crude product was extracted by using water and ethyl acetate. Over sodium sulfate, the organic ethyl acetate layer was dried and filtered. The excess of solvent was evaporated using a rota-evaporator to afford the required products. Further, the product was purified using column chromatography with hexane/ethyl acetate (70:30) mixture to give all pure compounds, **9a-9e** and **10a-10e**. Next, all these Boc-protected compounds were further deprotected using 20% trifluoroacetic acid (TFA) in DCM. The reaction mixture was stirred at 0 °C for 1 hour to obtain compounds **11a-11e** and **12a-12e**.

The structural and chemical makeup of the recently synthesized compounds were validated by spectroscopic methods (¹H NMR, ¹³C NMR and HRMS), and the spectra are shown in the supporting information (Figure S1–S50).

Tert-butyl ((2S,3S)-4-(4-(4-fluorophenyl)piperazin-1-yl)-3-hydroxy-1-phenylbutan-2-yl)carbamate (**4**). White solid, yield, 96%; mp 170–172 °C; ¹H NMR (400 MHz, CDCl₃): δ 7.33–7.17 (m, 5H), 6.94 (dd, *J* = 11.7, 5.7 Hz, 2H), 6.84 (dd, *J* = 9.2, 4.6 Hz, 2H), 4.99 (d, *J* = 9.7 Hz, 1H), 3.71 (dd, *J* = 12.9, 4.8 Hz, 2H), 3.08 (dd, *J* = 10.7, 6.7 Hz, 4H), 2.92 (dd, *J* = 15.4, 6.6 Hz, 2H), 2.75 (dd, *J* = 10.8, 5.0 Hz, 2H), 2.51 (dd, *J* = 9.9, 6.2 Hz, 3H), 2.28 (dd, *J* = 12.4, 3.2 Hz, 1H), 1.39 (s, 9H). ¹³C NMR (101 MHz, CDCl₃): δ 158.52, 155.92, 147.83, 138.40, 129.56, 128.49, 126.39, 117.93, 115.73, 115.51, 79.33, 65.43, 60.60, 53.17, 50.33, 39.53, 28.46.

Tert-butyl ((2S,3S)-3-hydroxy-1-phenyl-4-(4-(4-(trifluoromethyl)phenyl)piperazin-1-yl)butan-2-yl)carbamate (**5**). White solid, yield, 98%; mp 124–126 °C; ¹H NMR (400 MHz, CDCl₃): δ 7.46 (d, *J* = 8.7 Hz, 2H), 7.31–7.20 (m, 5H), 6.88 (d, *J* = 8.7 Hz, 2H), 5.00 (d, *J* = 9.7 Hz, 1H), 3.72 (d, *J* = 9.9 Hz, 2H), 3.23 (s, 4H), 2.99–2.87 (m, 2H), 2.73 (dd, *J* = 10.9, 5.0 Hz, 2H), 2.50 (dd, *J* = 10.8, 4.2 Hz, 2H), 2.28 (dd, *J* = 12.4, 3.1 Hz, 1H), 1.40 (s, 9H). ¹³C NMR (101 MHz, CDCl₃): δ 155.94, 153.22, 138.38, 129.56, 128.51, 126.42, 123.44, 120.60, 114.68, 79.37, 65.54, 60.68, 52.89, 48.14, 39.49, 28.45.

(2S,3S)-3-Amino-1-(4-(4-fluorophenyl)piperazin-1-yl)-4-phenylbutan-2-ol (**6**). White solid; mp 142–144 °C; yield, 71%; ¹H NMR (400 MHz, CDCl₃): δ 7.35–7.14 (m, 5H), 6.95 (t, *J* = 8.7 Hz, 2H), 6.88–6.82 (m, 2H), 3.74–3.60 (m, 1H), 3.17–3.05 (m, 4H), 2.95 (dd, *J* = 22.4, 6.7 Hz, 2H), 2.81 (td, *J* = 10.7, 4.2 Hz, 2H), 2.74–2.52 (m, 4H), 2.43 (dd, *J* = 12.3, 3.4 Hz, 2H). ¹³C NMR (101 MHz, CDCl₃): δ 158.51, 156.13, 147.88, 138.93, 129.41, 128.70, 126.54, 117.99, 115.52, 68.61, 68.59, 61.21, 55.96, 55.44, 53.42, 50.33, 41.32, 36.15.

(2S,3S)-3-Amino-4-phenyl-1-(4-(4-(trifluoromethyl)phenyl)piperazin-1-yl)butan-2-ol (**7**). White

solid; mp 129–131 °C; yield, 72%; ¹H NMR (400 MHz, CDCl₃): δ 7.47 (d, *J* = 8.7 Hz, 2H), 7.34–7.19 (m, 5H), 6.91 (d, *J* = 8.7 Hz, 2H), 3.66 (m, 1H), 3.27 (m, 4H), 2.91 (dd, *J* = 12.2, 8.9 Hz, 2H), 2.82–2.76 (m, 2H), 2.73–2.61 (m, 2H), 2.56 (dd, *J* = 12.5, 7.5 Hz, 2H), 2.42 (dd, *J* = 12.3, 3.5 Hz, 1H). ¹³C NMR (101 MHz, CDCl₃): δ 153.27, 139.13, 129.40, 128.67, 126.49, 123.45, 120.53, 114.64, 68.83, 61.29, 55.30, 53.12, 48.16, 41.66.

Tert-butyl ((S)-1-(((2S,3S)-4-(4-(4-fluorophenyl)piperazin-1-yl)-3-hydroxy-1-phenylbutan-2-yl)amino)-1-oxopropan-2-yl)carbamate (**9a**). White solid; mp 129–131 °C; yield, 52%; ¹H NMR (400 MHz, CDCl₃): δ 7.25 (q, *J* = 6.8 Hz, 5H), 7.19 (d, *J* = 6.5 Hz, 1H), 6.93 (t, *J* = 8.7 Hz, 2H), 6.83 (dd, *J* = 9.2, 4.6 Hz, 2H), 6.66 (d, *J* = 9.3 Hz, 1H), 4.90 (dd, *J* = 5.6, 2.5 Hz, 1H), 4.11–4.03 (m, 2H), 3.76 (dd, *J* = 11.0, 3.0 Hz, 1H), 3.06 (t, *J* = 4.8 Hz, 4H), 2.93 (d, *J* = 8.2 Hz, 2H), 2.77–2.72 (m, 2H), 2.57–2.48 (m, 3H), 2.28 (dd, *J* = 12.4, 3.2 Hz, 1H), 1.44 (s, 9H), 1.23 (d, *J* = 7.1 Hz, 3H). ¹³C NMR (101 MHz, CDCl₃): δ 172.54, 158.53, 156.15, 147.81, 138.05, 129.47, 128.49, 126.53, 117.94, 115.73, 80.20, 65.58, 60.10, 53.06, 51.20, 50.18, 38.99, 28.38, 18.30.

Tert-butyl ((S)-1-(((2S,3S)-4-(4-(4-fluorophenyl)piperazin-1-yl)-3-hydroxy-1-phenylbutan-2-yl)amino)-3-methyl-1-oxobutan-2-yl)carbamate (**9b**). White solid; mp 143–145 °C; yield, 56%; ¹H NMR (400 MHz, CDCl₃): δ 7.27–7.24 (m, 4H), 7.19 (dd, *J* = 7.9, 2.0 Hz, 1H), 6.96–6.90 (m, 2H), 6.82 (dd, *J* = 9.2, 4.6 Hz, 2H), 6.55 (d, *J* = 9.5 Hz, 1H), 4.86 (d, *J* = 7.2 Hz, 1H), 4.12 (dd, *J* = 17.3, 8.6 Hz, 1H), 3.90–3.83 (m, 1H), 3.75 (dd, *J* = 11.0, 3.0 Hz, 1H), 3.06 (t, *J* = 4.9 Hz, 4H), 2.95–2.72 (m, 4H), 2.58–2.44 (m, 3H), 2.21 (ddd, *J* = 19.0, 13.1, 4.3 Hz, 2H), 1.44 (s, 9H), 0.89 (d, *J* = 6.9 Hz, 3H), 0.73 (d, *J* = 6.9 Hz, 3H). ¹³C NMR (101 MHz, CDCl₃): δ 171.34, 158.52, 155.79, 147.79, 138.03, 129.43, 128.54, 126.54, 117.94, 115.51, 80.11, 65.58, 60.52, 53.05, 51.33, 50.21, 39.07, 30.11, 28.39, 19.52, 17.31.

Tert-butyl ((2S,3S)-1-(((2S,3S)-4-(4-(4-fluorophenyl)piperazin-1-yl)-3-hydroxy-1-phenylbutan-2-yl)amino)-3-methyl-1-oxopentan-2-yl)carbamate (**9c**). White solid; mp 157–159 °C; yield, 54%; ¹H NMR (400 MHz, CDCl₃): δ 7.28–7.17 (m, 5H), 6.97–6.91 (m, 2H), 6.83 (dd, *J* = 9.2, 4.6 Hz, 2H), 4.80 (d, *J* = 6.9 Hz, 1H), 4.13 (q, *J* = 8.1 Hz, 1H), 3.91 (dd, *J* = 7.3, 5.2 Hz, 1H), 3.74 (dd, *J* = 11.1, 3.1 Hz, 1H), 3.06 (t, *J* = 4.8 Hz, 4H), 2.94 (d, *J* = 7.9 Hz, 2H), 2.75 (dd, *J* = 11.0, 5.0 Hz, 2H), 2.59–2.39 (m, 4H), 2.27 (dd, *J* = 12.4, 3.2 Hz, 1H), 1.44 (s, 9H), 1.28–0.89 (m, 2H), 0.86–0.79 (m, 6H). ¹³C NMR (101 MHz, CDCl₃): δ 171.22, 158.52, 156.14, 147.83, 138.04, 129.43, 128.50, 126.52, 117.91, 115.72, 65.65, 60.08, 53.02, 51.20, 50.27, 39.11, 36.63, 28.38, 24.41, 15.89, 11.77.

Tert-butyl ((S)-1-(((2S,3S)-4-(4-(4-fluorophenyl)piperazin-1-yl)-3-hydroxy-1-phenylbutan-2-yl)amino)-1-oxo-3-phenylpropan-2-yl)carbamate (**9d**). White solid; mp 114–115 °C; yield, 54%; ¹H NMR (400 MHz, CDCl₃): δ 7.28 (dd, *J* = 13.8, 5.5 Hz, 5H), 7.19 (dd, *J* = 27.3, 7.7 Hz, 5H), 6.97–6.91 (m, 2H), 6.83 (dd, *J* = 9.2, 4.6 Hz, 2H), 6.49 (d, *J* = 9.1 Hz, 1H), 4.79 (d, *J* = 6.8 Hz, 1H), 4.28 (d, *J* = 6.7 Hz, 1H), 4.05 (dd, *J* = 16.9, 8.1 Hz, 1H), 3.67 (dd, *J* = 10.9, 3.1 Hz, 1H), 3.03 (dd, *J* = 9.0, 4.4 Hz, 4H), 2.96–2.83 (m, 4H), 2.71–2.63 (m, 2H), 2.51–2.41

(m, 2H), 2.32 – 2.10 (m, 2H), 1.40 (s, 9H). ¹³C NMR (101 MHz, CDCl₃): δ 171.06, 158.52, 156.14, 147.82, 138.06, 136.59, 129.35, 128.83, 127.10, 126.57, 117.98, 115.72, 80.35, 65.13, 59.89, 52.99, 51.39, 50.24, 38.97, 37.84, 28.33.

Tert-butyl (S)-2-(((2S,3S)-4-(4-(4-fluorophenyl)piperazin-1-yl)-3-hydroxy-1-phenylbutan-2-yl)carbamoyl)pyrrolidine-1-carboxylate (**9e**). White solid; mp 142-144 °C; yield, 53%; ¹H NMR (400 MHz, CDCl₃): δ 7.27 – 7.17 (m, 5H), 6.93 (t, *J* = 8.7 Hz, 2H), 6.83 (dd, *J* = 8.8, 4.2 Hz, 2H), 4.19 (dd, *J* = 8.3, 3.2 Hz, 1H), 4.14 (d, *J* = 7.9 Hz, 1H), 3.75 (d, *J* = 9.5 Hz, 1H), 3.29 (d, *J* = 10.7 Hz, 2H), 3.05 (s, 4H), 2.94 – 2.91 (m, 2H), 2.77 – 2.74 (m, 2H), 2.41 (dd, *J* = 125.1, 10.3 Hz, 4H), 1.93 – 1.89 (m, 2H), 1.67 (d, *J* = 40.7 Hz, 2H), 1.46 (s, 9H). ¹³C NMR (101 MHz, CDCl₃): δ 172.02, 158.50, 156.12, 147.88, 138.21, 129.38, 128.38, 126.44, 117.97, 117.90, 115.71, 115.49(s), 80.26, 66.05, 60.70, 59.77, 52.94, 50.79, 50.27, 47.29, 39.16, 29.78, 28.46, 24.32.

Tert-butyl ((S)-1-(((2S,3S)-3-hydroxy-1-phenyl-4-(4-(trifluoromethyl)phenyl)piperazin-1-yl)butan-2-yl)amino)-1-oxopropan-2-yl)carbamate (**10a**). White solid; mp 125-127 °C; yield, 51%; ¹H NMR (400 MHz, CDCl₃): δ 7.45 (d, *J* = 8.7 Hz, 2H), 7.32 – 7.16 (m, 5H), 6.88 (d, *J* = 8.7 Hz, 2H), 6.61 (d, *J* = 9.3 Hz, 1H), 4.79 (d, *J* = 4.9 Hz, 1H), 4.14 – 4.00 (m, 2H), 3.74 (dd, *J* = 11.1, 3.1 Hz, 1H), 3.21 (t, *J* = 5.0 Hz, 4H), 2.93 (d, *J* = 8.0 Hz, 2H), 2.76 – 2.68 (m, 2H), 2.55 – 2.22 (m, 4H), 1.44 (s, 9H), 1.23 (d, *J* = 7.2 Hz, 3H). ¹³C NMR (101 MHz, CDCl₃): δ 172.44, 155.33, 153.23, 138.04, 129.49, 129.46, 128.50, 126.55, 123.42, 120.93, 114.67, 80.25, 65.58, 60.00, 52.72, 51.05, 48.14, 39.04, 28.37, 18.26, 1.11.

Tert-butyl ((S)-1-(((2S,3S)-3-hydroxy-1-phenyl-4-(4-(trifluoromethyl)phenyl)piperazin-1-yl)butan-2-yl)amino)-3-methyl-1-oxobutan-2-yl)carbamate (**10b**). White solid; mp 191-193 °C; yield, 53%; ¹H NMR (400 MHz, CDCl₃): δ 7.44 (d, *J* = 8.2 Hz, 2H), 7.22 (dd, *J* = 29.4, 4.4 Hz, 5H), 6.87 (d, *J* = 8.2 Hz, 2H), 6.52 (t, *J* = 8.8 Hz, 1H), 4.82 (dd, *J* = 14.4, 7.2 Hz, 1H), 4.13 (d, *J* = 8.4 Hz, 1H), 3.89 – 3.83 (m, 1H), 3.76 (d, *J* = 9.9 Hz, 1H), 3.22 (s, 4H), 2.95 – 2.70 (m, 4H), 2.53 (s, 3H), 2.22 (dd, *J* = 55.2, 8.1 Hz, 2H), 1.44 (s, 9H), 0.88 (d, *J* = 11.1 Hz, 3H), 0.72 (d, *J* = 6.2 Hz, 3H). ¹³C NMR (101 MHz, CDCl₃): δ 171.29, 155.80, 153.22, 138.02, 129.47, 129.45, 129.43, 129.40, 128.55, 126.56, 126.48, 126.44, 114.67, 65.63, 60.52, 52.74, 51.21, 48.13, 39.09, 30.05, 28.38, 19.52, 17.27.

Tert-butyl ((2S,3S)-1-(((2S,3S)-3-hydroxy-1-phenyl-4-(4-(trifluoromethyl)phenyl)piperazin-1-yl)butan-2-yl)amino)-3-methyl-1-oxopentan-2-yl)carbamate (**10c**). White solid; mp 183-185 °C; yield, 53%; ¹H NMR (400 MHz, CDCl₃): δ 7.46 (d, *J* = 8.9 Hz, 2H), 7.35 – 7.16 (m, 5H), 6.88 (d, *J* = 8.8 Hz, 2H), 4.78 (d, *J* = 6.7 Hz, 1H), 4.19 – 4.07 (m, 1H), 3.92 (dd, *J* = 7.4, 5.0 Hz, 1H), 3.74 (dd, *J* = 10.9, 3.0 Hz, 1H), 3.22 (t, *J* = 4.9 Hz, 4H), 3.03 – 2.90 (m, 2H), 2.76 – 2.68 (m, 2H), 2.55 – 2.23 (m, 4H), 1.93 – 1.81 (m, 1H), 1.44 (s, 9H), 1.28 – 1.15 (m, 2H), 0.86 – 0.79 (m, 6H). ¹³C NMR (101 MHz, CDCl₃): δ 171.25, 155.75, 153.20, 138.00, 129.42, 128.77, 128.52, 126.45, 114.69, 80.14, 65.74, 64.91, 60.10, 52.73, 51.16, 48.11, 39.07, 36.58, 29.78, 28.37, 24.39, 15.89, 11.78.

Tert-butyl ((S)-1-(((2S,3S)-3-hydroxy-1-phenyl-4-(4-(trifluoromethyl)phenyl)piperazin-1-yl)butan-2-yl)amino)-1-

oxo-3-phenylpropan-2-yl)carbamate (**10d**). White solid; mp 190-192 °C; yield, 54%; ¹H NMR (400 MHz, CDCl₃): δ 7.46 (d, *J* = 8.7 Hz, 2H), 7.32 – 7.14 (m, 10H), 6.88 (d, *J* = 8.7 Hz, 2H), 6.50 (d, *J* = 9.2 Hz, 1H), 4.79 (d, *J* = 6.9 Hz, 1H), 4.29 (d, *J* = 6.8 Hz, 1H), 4.06 (dd, *J* = 16.8, 8.1 Hz, 1H), 3.68 (d, *J* = 10.8 Hz, 1H), 3.20 (t, *J* = 5.0 Hz, 4H), 3.04 – 2.87 (m, 4H), 2.68 (dd, *J* = 11.2, 5.2 Hz, 2H), 2.47 (dd, *J* = 10.6, 5.0 Hz, 2H), 2.34 – 2.10 (m, 2H), 1.41 (s, 9H). ¹³C NMR (101 MHz, CDCl₃): δ 171.11, 153.19, 138.02, 136.57, 129.49, 128.84, 127.11, 126.59, 123.41, 120.98, 114.68, 65.22, 59.95, 56.15, 52.89, 52.71, 52.59, 51.36, 48.13, 48.08, 38.93, 29.78, 28.32.

Tert-butyl (S)-2-(((2S,3S)-3-hydroxy-1-phenyl-4-(4-(trifluoromethyl)phenyl)piperazin-1-yl)butan-2-yl)carbamoyl)pyrrolidine-1-carboxylate (**10e**). White solid; mp 167-169 °C; yield, 52%; ¹H NMR (400 MHz, CDCl₃): δ 7.46 (d, *J* = 8.7 Hz, 2H), 7.24 (q, *J* = 6.8 Hz, 5H), 6.89 (d, *J* = 8.7 Hz, 2H), 6.78 (d, *J* = 9.1 Hz, 1H), 4.20 (dd, *J* = 8.4, 3.0 Hz, 1H), 3.77 (dd, *J* = 22.0, 12.9 Hz, 1H), 3.35 – 3.28 (m, 1H), 3.22 (s, 4H), 3.02 – 2.70 (m, 4H), 2.64 – 2.52 (m, 2H), 2.18 (dd, *J* = 66.0, 28.8 Hz, 2H), 1.93 (dd, *J* = 18.7, 7.4 Hz, 2H), 1.74 (s, 2H), 1.47 (s, 9H). ¹³C NMR (101 MHz, CDCl₃): δ 172.10, 155.29, 153.22, 138.20, 129.38, 128.39, 126.43, 126.12, 123.43, 114.67, 80.26, 66.13, 60.71, 59.76, 52.67, 50.79, 48.07, 47.31, 39.12, 31.74, 29.78, 28.45, 24.29.

(S)-2-Amino-N-((2S,3S)-4-(4-(4-fluorophenyl)piperazin-1-yl)-3-hydroxy-1-phenylbutan-2-yl)propanamide (**11a**). White solid; mp 149-151 °C; yield, 51%; ¹H NMR (400 MHz, CDCl₃): δ 7.48 (d, *J* = 9.6 Hz, 1H), 7.26 (dd, *J* = 9.5, 5.0 Hz, 5H), 6.94 (t, *J* = 8.7 Hz, 2H), 6.84 (dd, *J* = 9.1, 4.6 Hz, 2H), 4.07 (dd, *J* = 16.8, 8.7 Hz, 1H), 3.78 (dd, *J* = 10.0, 3.1 Hz, 1H), 3.43 (dd, *J* = 15.4, 8.4 Hz, 1H), 3.07 (s, 4H), 2.96 (dd, *J* = 7.8, 2.6 Hz, 2H), 2.76 – 2.72 (m, 2H), 2.51 – 2.46 (m, 2H), 2.35 (dt, *J* = 12.4, 10.6 Hz, 2H), 1.14 (d, *J* = 7.0 Hz, 3H). ¹³C NMR (101 MHz, CDCl₃): δ 175.76, 156.14, 147.86, 138.21, 129.51, 128.47, 118.04, 66.21, 60.84, 53.20, 51.32, 50.89, 50.34, 39.02, 21.85.

(S)-2-Amino-N-((2S,3S)-4-(4-(4-fluorophenyl)piperazin-1-yl)-3-hydroxy-1-phenylbutan-2-yl)-3-methylbutanamide (**11b**). White solid; mp 154-156 °C; yield, 54%; ¹H NMR (400 MHz, CDCl₃): δ 7.57 (d, *J* = 9.6 Hz, 1H), 7.26 – 7.25 (m, 4H), 7.17 (dd, *J* = 9.6, 4.5 Hz, 1H), 6.95 – 6.91 (m, 2H), 6.84 – 6.81 (m, 2H), 4.12 (q, *J* = 8.5 Hz, 1H), 3.79 (dd, *J* = 10.4, 3.6 Hz, 1H), 3.16 (d, *J* = 3.9 Hz, 1H), 3.08 – 3.05 (m, 4H), 2.95 (dd, *J* = 7.8, 2.7 Hz, 2H), 2.76 – 2.71 (m, 2H), 2.51 – 2.34 (m, 4H), 2.22 – 2.17 (m, 1H), 0.87 (d, *J* = 7.0 Hz, 3H), 0.55 (d, *J* = 6.9 Hz, 3H). ¹³C NMR (101 MHz, CDCl₃): δ 170.02, 158.55, 156.17, 147.77, 138.07, 129.46, 128.57, 126.58, 117.96, 115.76, 65.40, 60.70, 53.17, 51.63, 50.89, 50.29, 39.12, 23.51.

(2S,3S)-2-Amino-N-((2S,3S)-4-(4-(4-fluorophenyl)piperazin-1-yl)-3-hydroxy-1-phenylbutan-2-yl)-3-methylpentanamide (**11c**). White solid; mp 158-160 °C; yield, 51%; ¹H NMR (400 MHz, CDCl₃): δ 7.57 (d, *J* = 9.6 Hz, 1H), 7.26 (dd, *J* = 5.2, 2.0 Hz, 4H), 7.19 (dd, *J* = 10.0, 4.3 Hz, 1H), 6.94 (t, *J* = 8.7 Hz, 2H), 6.86 – 6.82 (m, 2H), 4.13 (q, *J* = 8.9 Hz, 1H), 3.79 (dd, *J* = 9.8, 4.3 Hz, 1H), 3.20 (d, *J* = 3.8 Hz, 1H), 3.09 – 3.06 (m, 4H), 2.96 (dd, *J* = 7.9, 1.9 Hz, 2H), 2.78 – 2.73 (m, 2H), 2.52 – 2.32 (m, 4H), 1.89 (dd, *J* = 9.5, 6.9 Hz, 1H), 0.91 (dd, *J* = 21.1, 8.2 Hz,

1H), 0.84 (d, $J = 7.0$ Hz, 3H), 0.76 (t, $J = 7.1$ Hz, 3H). ^{13}C NMR (101 MHz, CDCl_3): δ 156.15(s), 147.80, 138.09, 129.45, 128.56, 126.57, 118.02, 115.74, 115.74, 66.54, 65.41, 60.69, 53.17, 51.61, 51.47, 50.32, 39.14, 37.67, 23.51, 23.16, 16.17, 11.98.

(S)-2-Amino-N-((2S,3S)-4-(4-(4-fluorophenyl)piperazin-1-yl)-3-hydroxy-1-phenylbutan-2-yl)-3-phenylpropanamide (**11d**). White solid; mp 147-149 °C; yield, 56%; ^1H NMR (400 MHz, CDCl_3): δ 7.55 (d, $J = 9.6$ Hz, 1H), 7.32 – 7.27 (m, 5H), 7.26 – 7.13 (m, 5H), 6.97 – 6.92 (m, 2H), 6.86 – 6.82 (m, 2H), 4.14 – 4.07 (m, 1H), 3.80 (dd, $J = 10.5, 2.8$ Hz, 1H), 3.55 (dd, $J = 9.5, 4.2$ Hz, 1H), 3.11 – 3.07 (m, 4H), 2.95 (dd, $J = 7.8, 2.6$ Hz, 2H), 2.81 – 2.75 (m, 2H), 2.56 – 2.49 (m, 2H), 2.44 – 2.31 (m, 4H). ^{13}C NMR (101 MHz, CDCl_3): δ 174.39, 163.42, 158.58, 156.20, 147.76, 138.08, 129.57, 128.79, 126.87, 118.01, 115.55, 66.12, 60.79, 56.70, 53.18, 51.53, 50.17, 40.97, 38.95.

(S)-N-((2S,3S)-4-(4-(4-Fluorophenyl)piperazin-1-yl)-3-hydroxy-1-phenylbutan-2-yl)pyrrolidine-2-carboxamide (**11e**). White solid; mp 143-145 °C; yield, 52%; ^1H NMR (400 MHz, CDCl_3): δ 7.84 (d, $J = 9.8$ Hz, 1H), 7.27 – 7.19 (m, 5H), 6.96 – 6.91 (m, 2H), 6.83 (dd, $J = 9.2, 4.6$ Hz, 2H), 4.10 (dd, $J = 16.5, 9.1$ Hz, 1H), 3.79 (dd, $J = 10.0, 4.1$ Hz, 1H), 3.65 (dd, $J = 9.4, 4.9$ Hz, 1H), 3.06 (d, $J = 2.5$ Hz, 4H), 2.93 – 2.89 (m, 2H), 2.78 – 2.75 (m, 2H), 2.73 – 2.67 (m, 2H), 2.52 – 2.32 (m, 4H), 1.99 – 1.94 (m, 1H), 1.57 – 1.48 (m, 2H), 1.37 (dt, $J = 56.8, 32.1$ Hz, 2H). ^{13}C NMR (101 MHz, CDCl_3): δ 175.36, 156.10, 147.87, 138.29, 129.41, 128.42, 126.46, 117.90, 115.72, 66.83, 60.83, 60.56, 53.19, 51.11, 50.34, 47.32, 38.96, 30.80, 26.09.

(S)-2-Amino-N-((2S,3S)-3-hydroxy-1-phenyl-4-(4-(4-(trifluoromethyl)phenyl)piperazin-1-yl)butan-2-yl)propanamide (**12a**). White solid; mp 134-136 °C; yield, 51%; ^1H NMR (400 MHz, CDCl_3): δ 7.51 (d, $J = 9.5$ Hz, 1H), 7.46 (d, $J = 8.7$ Hz, 2H), 7.33 – 7.16 (m, 6H), 6.88 (d, $J = 8.7$ Hz, 2H), 4.08 (q, $J = 8.3$ Hz, 1H), 3.80 (d, $J = 12.8$ Hz, 1H), 3.45 (q, $J = 6.8$ Hz, 1H), 3.24 (s, 4H), 2.96 (dd, $J = 7.7, 3.1$ Hz, 2H), 2.75 (dd, $J = 10.8, 5.5$ Hz, 2H), 2.53 – 2.35 (m, 4H), 1.15 (d, $J = 6.9$ Hz, 3H). ^{13}C NMR (101 MHz, CDCl_3): δ 175.62, 153.14, 138.17, 129.49, 128.49, 126.53, 126.51, 126.47, 120.71, 114.74, 66.28, 60.89, 52.91, 51.43, 50.86, 48.05, 38.92, 21.70.

(S)-2-Amino-N-((2S,3S)-3-hydroxy-1-phenyl-4-(4-(4-(trifluoromethyl)phenyl)piperazin-1-yl)butan-2-yl)-3-methylbutanamide (**12b**). White solid; mp 153-155 °C; yield, 55%; ^1H NMR (400 MHz, CDCl_3): δ 7.60 (d, $J = 9.5$ Hz, 1H), 7.44 (d, $J = 8.5$ Hz, 2H), 7.25 (dd, $J = 7.6, 5.6$ Hz, 5H), 7.20 – 7.14 (m, 1H), 6.87 (d, $J = 8.4$ Hz, 2H), 4.12 (q, $J = 8.5$ Hz, 1H), 3.80 (d, $J = 10.3$ Hz, 1H), 3.25 – 3.15 (m, 5H), 3.00 – 2.91 (m, 2H), 2.74 (dd, $J = 10.0, 4.1$ Hz, 2H), 2.52 – 2.32 (m, 4H), 2.25 – 2.15 (m, 1H), 0.86 (d, $J = 7.0$ Hz, 3H), 0.55 (d, $J = 6.9$ Hz, 3H). ^{13}C NMR (101 MHz, CDCl_3): δ 174.39, 153.17, 138.25, 129.42, 128.54, 126.52, 123.40, 120.69, 114.72, 66.52, 60.95, 60.28, 52.93, 51.55, 48.10, 38.99, 30.64, 19.76, 15.67.

(2S,3S)-2-Amino-N-((2S,3S)-3-hydroxy-1-phenyl-4-(4-(4-(trifluoromethyl)phenyl)piperazin-1-yl)butan-2-yl)-3-methylpentanamide (**12c**). White solid; mp 121-123 °C; yield, 55%; ^1H NMR (400 MHz, CDCl_3): δ 7.68 (s, 1H), 7.46 (d, $J = 8.7$ Hz, 2H), 7.22 (dt, $J = 8.4, 4.5$ Hz, 5H), 6.88 (d, $J = 8.7$ Hz, 2H), 4.15 (q, $J = 9.2$ Hz, 1H), 3.86 (d, $J = 11.3$ Hz, 1H), 3.28 (s,

5H), 3.00 – 2.78 (m, 4H), 2.69 – 2.39 (m, 4H), 2.04 – 1.83 (m, 2H), 0.97 (s, 1H), 0.78 (dd, $J = 19.9, 7.1$ Hz, 6H). ^{13}C NMR (101 MHz, CDCl_3): δ 174.33, 153.11, 138.21, 129.43, 128.53, 126.52, 123.40, 121.09, 114.76, 66.62, 60.93, 60.06, 52.90, 51.60, 47.99, 38.92, 37.68, 23.23, 16.10, 11.95. m/z: (M+) calcd for $\text{C}_{27}\text{H}_{37}\text{F}_3\text{N}_4\text{O}_2$: 506.2869; found: 506.2868.

(S)-2-Amino-N-((2S,3S)-3-hydroxy-1-phenyl-4-(4-(4-(trifluoromethyl)phenyl)piperazin-1-yl)butan-2-yl)-3-phenylpropanamide (**12d**). White solid; mp 143-145 °C; yield, 54%; ^1H NMR (400 MHz, CDCl_3): δ 7.55 (d, $J = 9.6$ Hz, 1H), 7.46 (d, $J = 8.8$ Hz, 2H), 7.29 (dd, $J = 6.9, 3.2$ Hz, 5H), 7.19 (dd, $J = 33.2, 8.1$ Hz, 5H), 6.89 (d, $J = 8.8$ Hz, 2H), 4.11 (q, $J = 9.0$ Hz, 1H), 3.84 – 3.74 (m, 1H), 3.54 (dd, $J = 9.5, 4.2$ Hz, 1H), 3.23 (s, 4H), 3.02 (ddd, $J = 14.2, 10.6, 5.2$ Hz, 4H), 2.76 – 2.68 (m, 2H), 2.51 – 2.41 (m, 2H), 2.38 – 2.31 (m, 2H). ^{13}C NMR (101 MHz, CDCl_3): δ 174.35, 153.21, 138.24, 129.56, 128.52, 126.59, 114.69, 66.18, 60.88, 56.69, 52.91, 51.48, 48.15, 40.97, 39.00.

(S)-N-((2S,3S)-3-Hydroxy-1-phenyl-4-(4-(4-(trifluoromethyl)phenyl)piperazin-1-yl)butan-2-yl)pyrrolidine-2-carboxamide (**12e**). White solid; mp 154-156 °C; yield, 53%; ^1H NMR (400 MHz, CDCl_3): δ 7.85 (d, $J = 9.7$ Hz, 1H), 7.47 (d, $J = 8.6$ Hz, 2H), 7.30 – 7.26 (m, 2H), 7.24 (s, 2H), 7.20 (d, $J = 8.3$ Hz, 1H), 6.90 (d, $J = 8.6$ Hz, 2H), 4.12 (q, $J = 8.6$ Hz, 1H), 3.82 (d, $J = 10.0$ Hz, 1H), 3.68 (dd, $J = 9.2, 4.9$ Hz, 1H), 3.25 (s, 4H), 3.03 – 2.89 (m, 3H), 2.74 (dt, $J = 16.3, 6.4$ Hz, 3H), 2.54 – 2.35 (m, 4H), 1.99 (dd, $J = 13.2, 8.1$ Hz, 1H), 1.62 – 1.23 (m, 4H). ^{13}C NMR (101 MHz, CDCl_3): δ 175.28, 153.16, 138.19, 129.31, 128.35, 126.39, 123.36, 120.51, 114.59, 66.86, 60.52, 52.86, 51.10, 48.08, 47.23, 38.84, 30.71, 25.99. m/z: (M+) calcd for $\text{C}_{26}\text{H}_{33}\text{F}_3\text{N}_4\text{O}_2$: 490.2556; found: 490.2556.

Biology

Parasite culture

Pf3D7 was developed using the techniques outlined by Trager and Jensen.¹⁶ Human O+ RBCs were utilized to grow parasites in a complete medium consisting of complete RPMI 1640 containing NaHCO_3 , AlbuMax II, hypoxanthine and gentamicin. At a temperature of 37 °C, parasites were grown in a gas mixture containing 5% O_2 , 5% CO_2 , and 90% N_2 . To establish whether there were any parasites, Giemsa-stained blood smears were scored. Bright-field microscopy examination was used to check the efficacy of the compounds at various dosages against *Pf3D7*.

MTT assay

The MTT test, a colorimetric assay based on the measurement of cell metabolic activity, was performed to determine the *in vitro* cytotoxicity of the listed compounds against the HepG2 cell line.¹⁷ The compounds that were synthesized underwent a triple analysis. HepG2 cells were raised in sterile culture flasks at a temperature of 37 °C and CO_2 using a DMEM medium supplemented with FBS and gentamicin (40 mg/mL). The media were changed three times per week. The cells were then divided into 96-well plates with 5000 cells per well, trypsinized, cleaned, and resuspended in complete media before being treated for an additional 24 hours at 37 °C. After 48 hours of incubation at 37 °C, the supernatant was taken out, and 100 μL of the MTS solution in full DMEM was introduced to each well. The next step was a two-hour incubation period at 37 °C. The experimental culture

plates were analysed using a OD meter and an absorbance measurement at 450 nm (Tecan Infinite M200, Nanoquant, UK). Excel (software) was used to analyze the data and determine cytotoxicity.

Computational Studies

Molecular Docking and MMGBSA

Prior to molecular docking investigations with the already synthesized compounds (**12c** and **12e**), the target proteins were improved and prepared. According to our previously published works of literature, all the procedures, including protein preparation, ligand production, molecular docking, and binding free energy calculation, were carried out using Schrödinger (Schrödinger Release 2021-1) software.^{18,19}

Physicochemical properties

SWISS ADME²⁰ and Molsoft L.L.C.²¹ were used to calculate the ADME profile of all the designed and synthesized compounds. Molecular weight, H-bond acceptors, H-bond donors, anticipated octanol/water partition coefficient (MLogP), TPSA (Total Polar Surface Area), Lipinski violation, drug-likeness score, and BBB value are some of the predicted ADME features.

RESULT AND DISCUSSION

Chemistry

Twenty novel fluorinated piperazine based amino acids hybrid analogues (**9a-9e**, **10a-10e**, **11a-11e**, and **12a-12e**) were synthesized using a three-step synthetic process to develop potent antimalarial scaffolds (Scheme 1 and Figure 1). Initially, to synthesise Boc-protected HEA precursors (**4-5**), we followed, a convenient microwave-assisted ring opening of *tert*-butyl ((*S*)-1-((*R*)-oxiran-2-yl)-2-phenylethyl)carbamate (**1**) in the presence of substituted piperazine (**2-3**). These products (**4-5**), were then

subjected to isolate compounds **6** and **7** by deprotection of the Boc group using TFA in dichloromethane.

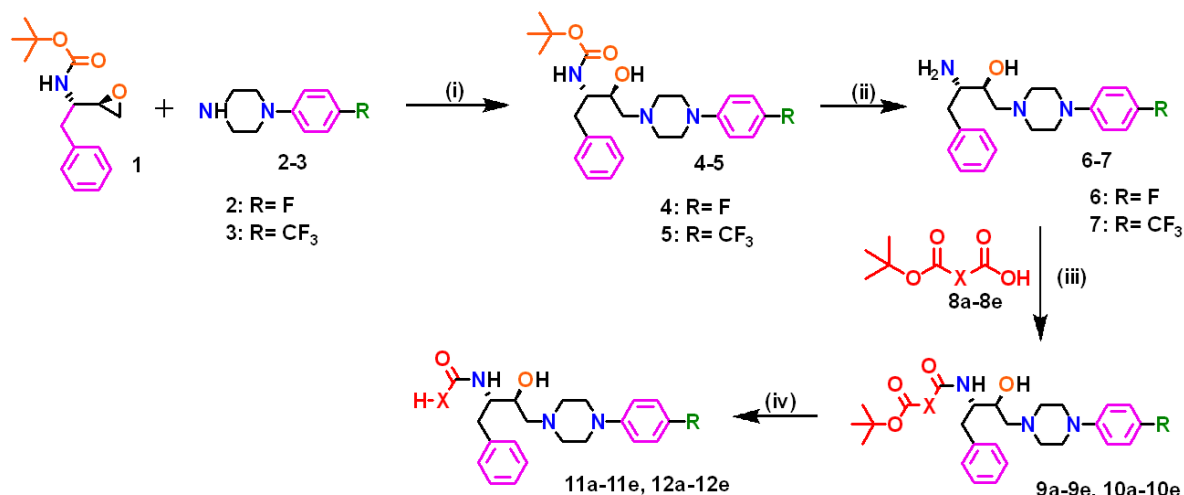
To explore Structure-Activity relationship (SAR), modifications were performed with different Boc-amino acids **8a-8e** (Boc-alanine **8a**, Boc-valine **8b**, Boc-isoleucine **8c**, Boc-phenylalanine **8d**, and Boc-proline **8e**) to yield Boc-protected novel analogues, **9a-9e** and **10a-10e**. Further, these novel analogues **9a-9e** and **10a-10e** were deprotected using TFA in DCM to afford **11a-11e** and **12a-12e** containing free -NH₂ groups. The chemical composition of all the synthesized compounds was confirmed by different spectroscopic techniques (¹H-NMR, ¹³C-NMR and HRMS).

Biology

Cytotoxicity and Growth Inhibition Assay

Initially, to evaluate the cytotoxicity of all the listed compounds on human liver cells (HepG2), an MTT assay was carried out. All the compounds showed a TC₅₀ value of >100 μM (Table 1, Figure 2). To prioritize candidates for further investigations, the initial screening for synthesized fluorinated, N-(3-hydroxy-1-phenyl-4-(4-phenylpiperazin-1-yl)alkyl)amides containing different amino acids, **9a-9e**, **10a-10e**, **11a-11e**, and **12a-12e** was conducted to assess their *in-vitro* anti-plasmodium activity against the blood stage (BS).

The efficacy of compounds was evaluated at two different concentrations, 1 μM, and 5 μM, against CQ-sensitive strain (*Pf3D7*) of the malaria parasite by using a synchronized culture with ART as a positive control (Table 1). Among all the compounds, ten compounds (**11a-11e**, **12a-12e**) showed more than 60% inhibition at 5 μM with two derivatives as hits **12c** and **12e** (Figure 3).



Compound	a	b	c	d	e
X					

Scheme 1. Synthesis of analogues, **9a-9e**, **10a-10e**, **11a-11e**, and **12a-12e**. Conditions: i) microwave, 300W, 40 min, 70 °C, ethanol ii) 20% TFA in DCM, 2 h iii) TEA, DCM, EDC.HCl, HOBt, 0 °C to RT, 24 h iv) 20% TFA in DCM, 2 h.

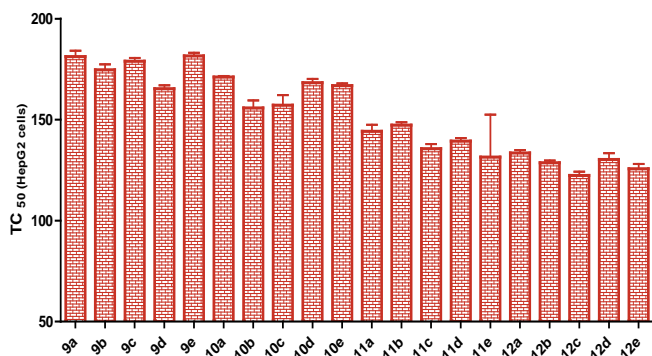


Figure 2. TC₅₀ of all the synthesized novel analogues against the HepG2 cell line.

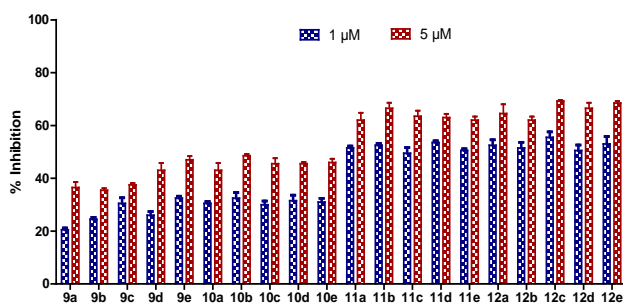


Figure 3. Percentage inhibition of all the synthesized analogues at 1 μM and 5 μM concentration against *Pf3D7*.

Further, hits (**12c** and **12e**) were evaluated for IC₅₀ determination with positive control of ART (4nM) and displayed IC₅₀ values of $0.696 \pm 0.0462 \mu\text{M}$ and $0.9377 \pm 0.0461 \mu\text{M}$, respectively against *Pf3D7* strain of malaria parasite. Next, a combination assay was performed to investigate the behavior of these hits along with ART. The growth inhibition experiment of hits **12c** and **12e** in combination with ART (1nM), against the *Pf3D7* strain of the malaria parasite was carried out at their IC₅₀ values (Figure 4). Compared to each hit molecule being individually treated, the combined action was slightly better for both compounds with IC₅₀ values of $0.19 \mu\text{M}$ (**12c** + ART) and $0.26 \mu\text{M}$ (**12e** + ART) as shown in Figure 4. Overall, both compounds showed an additive effect in combination with ART.

Computational Studies: Molecular docking and MMGBSA

A computational study was used to assess the ADME profiles of the hit compounds to determine their drug-likeness. With few exceptions in terms of molecular weight, as indicated in Table S1; supplementary information, all the compounds demonstrated good physiochemical properties necessary for developing a therapeutic molecule. Further, we were keen to explore the identified hits (**12c** and **12e**) for *in-silico* studies. Plasmepsins are a family of aspartic proteases that are involved in the processing of proteins during the life cycle of the parasite. Plasmepsin V is primarily involved in the maturation of the parasite's gametocytes, which are the sexual stage of the parasite that is

responsible for transmission to mosquitoes. Plasmepsin X, on the other hand, is involved in the degradation of haemoglobin in the food vacuole of the parasite. Both plasmepsin V and X have been identified as potential drug targets for the treatment of malaria.

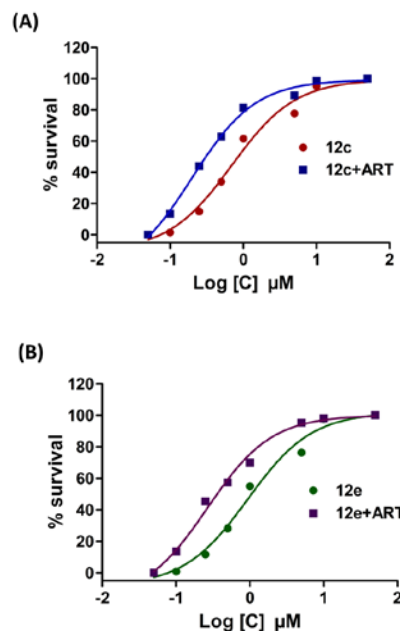
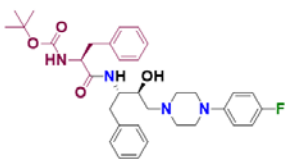
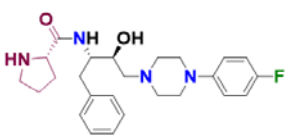
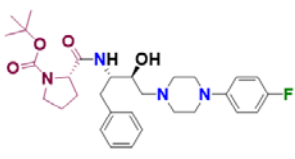
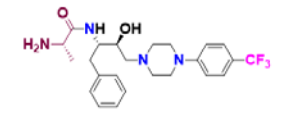
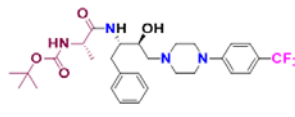
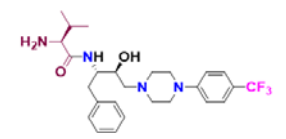
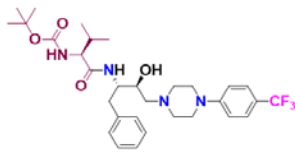
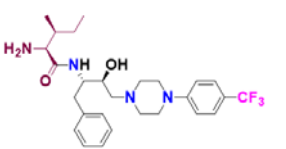
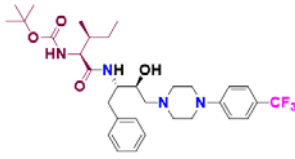
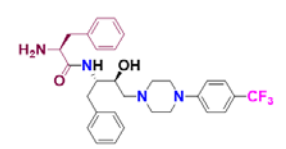
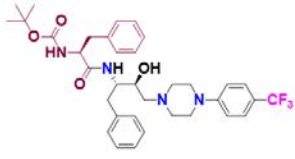
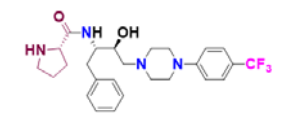
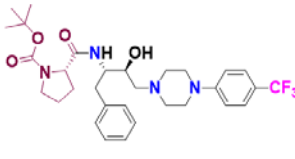
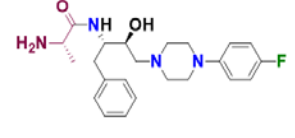
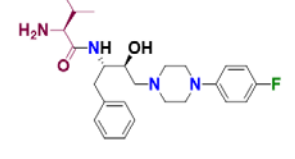
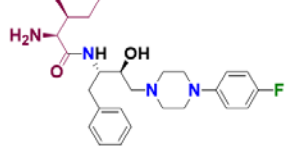
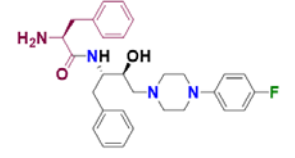


Figure 4. A) Curve showing the percent inhibition of compound **12c** alone (red curve) and in combination with ART (blue curve); B) Curve showing the percent inhibition of compound **12e** alone (purple curve) and in combination with ART (green curve).

Table 1. *In vitro* antiplasmodial activity and cytotoxicity of synthesized analogues **9a-9e**, **10a-10e**, **11a-11e**, and **12a-12e**.

Entry Code No.	Compound	ABS ^a (~ % Inhibition in μM, <i>Pf3D7</i>)		Cytotoxicity TC ₅₀ μM (HepG2 cells)
		1 μM	5 μM	
1. 9a		21	38	181.2
2. 9b		24	36	174.7
3. 9c		29	38	178.9

4.	9d		27	41	165.3	15	11e		51	63	131.5																												
5.	9e		32	48	181.6	16	12a		54	67	133.5																												
6.	10a		31	45	171.1	17	12b		50	61	128.7																												
7.	10b		34	48	155.8	18	12c		54	69	122.4																												
8.	10c		29	47	157.2	19	12d		52	68	130.3																												
9.	10d		33	46	168.3	20	12e		55	69	125.7																												
10.	10e		30	47	166.9	<p>^a ABS, asexual blood stage; % inhibitions represent means from n values of ≥ 2 independent experiments.</p> <p>Table 2. Docking score and binding free energy for compounds 12c and 12e against two Plms, Plm V and Plm X.</p> <table border="1"> <thead> <tr> <th rowspan="2">Entry No.</th> <th rowspan="2">Compound</th> <th colspan="2">Plm V</th> <th colspan="2">Plm X</th> </tr> <tr> <th>Docking Score</th> <th>MMGBSA</th> <th>Docking Score</th> <th>MMGBSA</th> </tr> </thead> <tbody> <tr> <td>1</td> <td>12c</td> <td>-8.447</td> <td>-57.56</td> <td>-5.294</td> <td>-54.74</td> </tr> <tr> <td>2</td> <td>12e</td> <td>-8.095</td> <td>-54.16</td> <td>-5.268</td> <td>-49.76</td> </tr> <tr> <td>3</td> <td>ART</td> <td>-2.974</td> <td>-42.59</td> <td>-4.089</td> <td>-43.08</td> </tr> </tbody> </table>						Entry No.	Compound	Plm V		Plm X		Docking Score	MMGBSA	Docking Score	MMGBSA	1	12c	-8.447	-57.56	-5.294	-54.74	2	12e	-8.095	-54.16	-5.268	-49.76	3	ART	-2.974	-42.59	-4.089	-43.08
Entry No.	Compound	Plm V		Plm X																																			
		Docking Score	MMGBSA	Docking Score	MMGBSA																																		
1	12c	-8.447	-57.56	-5.294	-54.74																																		
2	12e	-8.095	-54.16	-5.268	-49.76																																		
3	ART	-2.974	-42.59	-4.089	-43.08																																		
11.	11a		52	64	144.2																																		
12.	11b		53	68	147.3																																		
13.	11c		51	65	135.6																																		
14.	11d		53	64	139.4																																		

^a ABS, asexual blood stage; % inhibitions represent means from n values of ≥ 2 independent experiments.

Table 2. Docking score and binding free energy for compounds **12c** and **12e** against two Plms, Plm V and Plm X.

Entry No.	Compound	Plm V		Plm X	
		Docking Score	MMGBSA	Docking Score	MMGBSA
1	12c	-8.447	-57.56	-5.294	-54.74
2	12e	-8.095	-54.16	-5.268	-49.76
3	ART	-2.974	-42.59	-4.089	-43.08

Plasmeppsin V and X are two enzymes that are essential for the survival of the malaria parasite and hence been identified as potential drug targets for the treatment of malaria. Keeping these facts under consideration, both identified hits (**12c** and **12e**) were docked with two Plms (V and X), as represented in Table 2. The results of both the ligands were also compared with the positive control ART (Table 2, entry 3), however, the data suggested that both compounds showed much better computational results compared to ART against Plms (V and X).

The results of the molecular interaction analysis with each Plm V and X in terms of docking score and MMGBSA (Molecular Mechanics/Generalized Born Surface Area) are shown in Figure 5-6. MMGBSA calculates the binding free energy of a protein-ligand complex as the difference between the free energy of the complex and the sum of the free energies of the isolated protein

and ligand. Overall, both drug candidates performed well when evaluated based on their molecular interactions with various amino acid residues of Plms, binding free energy (measured in Kcal/mol), and docking score (measured in Kcal/mol).

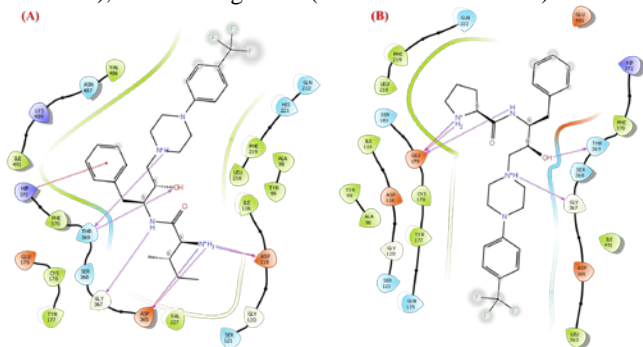


Figure 5. Docking pose of (A) **12c** (displayed one pi cation with residue Hip_372, five H-bond with residues Asp_118, Asp_365, Gly_367, and twice with Thr_369); and (B) **12e** (displayed four H-bond interactions with residues twice with Glu_179, Gly_367, and Thr_369) with Plm V.

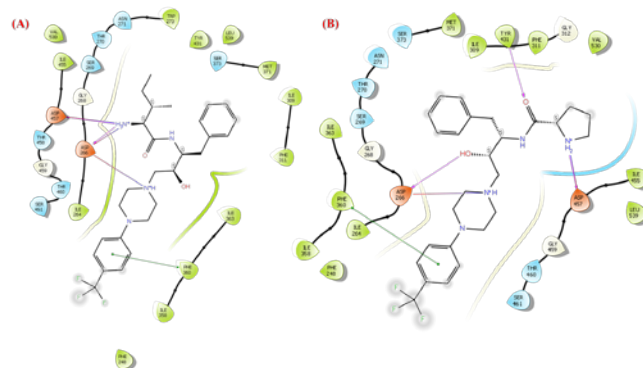


Figure 6. Docking pose of (A) **12c** (displayed one pi-pi stacking with residue Phe_360, two H-bond with residues Asp_266, and Asp_457); and (B) **12e** (displayed one pi-pi stacking with residue Phe_360, three H-bond with residues Asp_266, Asp_457, and Tyr_431) with Plm X.

Altogether, the *in-silico* studies were found to be in support of *in-vitro* results. Notably, compound **12c** demonstrated superior binding performance based on better molecular interactions, docking score, and binding free energy (Table 2, entry 1) as compared to compound **12e** with both Plm V and Plm X (Figures 5 and 6). Further, more studies related to enzymatic assays need to be performed to comment on the target of these two hits.

CONCLUSION

Twenty novel analogues of fluorinated, N-(3-hydroxy-1-phenyl-4-(4-phenylpiperazin-1-yl)alkyl)amides containing different amino acids were designed and synthesized using a convenient synthetic approach. The novel compounds (**9a-9e**, **10a-10e**, **11a-11e**, and **12a-12e**) were tested on the HepG2 cell line using the MTT viability assay. All compounds were non-toxic up to 100 μ M. After cytotoxicity, initial screening of all the compounds was performed at two different concentrations 1 μ M and 5 μ M, against *Pf3D7* strain of malaria parasite. As a result,

two hits **12c** and **12e** showed efficacy against the chloroquine-sensitive *Pf3D7* strain with IC_{50} values of $0.696 \pm 0.0462 \mu$ M and $0.9377 \pm 0.0461 \mu$ M, respectively. To examine the combinatorial effect of **12c** and **12e**, an *in-vitro* combination assay with ART was also performed. When combined with ART (1nM), both hit additively affect parasite growth inhibition. Additionally, the docking experiments showed a close correlation between the antimalarial activities and their interaction energies with Plm V and Plm X, suggesting that these Plms may be the likely target(s) for these hit molecules, **12c** and **12e**.

ACKNOWLEDGMENT

Poonam and BR thank the Science & Engineering Research Board for the financial support (CRG/2020/005800). Department of Science and Technology, Government of India, for financial support (DST/TDT/AGRO-54/2021). CU and SK are highly grateful to CSIR for the senior research fellowship. SB is grateful to NII for the senior research fellowship.

Declarations. All the photos and graphics used in the manuscript are original, created by the authors, and not submitted anywhere else for publication.

Author contribution. Concept: Poonam, BR, and APS; Synthesis, chemical, and physical characterization: CU, DK, NB, BR, and Poonam; Antimalarial and cytotoxicity assays: CU and SB and APS; Molecular docking and ADME: CU, NB and SK. All the authors contributed to writing the manuscript and approved it for submission.

Conflict of Interest: The authors declare no conflict of interest.

Abbreviation used

CQ: Chloroquine
WHO: World Health Organization
 IC_{50} : Half-maximal inhibitory concentration;
 TC_{50} : Median toxic concentration
MTT: (3-(4,5-Dimethylthiazol-2-yl)-2,5-Diphenyltetrazolium Bromide)
DCM: Dichloromethane
Pf: Plasmodium falciparum
Boc: Tert-butyloxycarbonyl
EDC.HCl: 1-(3-dimethylaminopropyl)-3-ethylcarbodiimide hydrochloride
HOBt: Hydroxybenzotriazole
ADME: Absorption, distribution, metabolism, and excretion;
NMR: Nuclear magnetic resonance

REFERENCES

1. J. Yang, Y. Wang, W. Guan *et. al.* Spiral molecules with antimalarial activities: A review. *Eur. Jour. Med. Chem.* **2022**, 237114361.
2. A.L. Abner. A Global Issue: the Malaria Epidemic in Africa. **2014**.
3. Á.F. Chora, M.M. Mota, M. Prudêncio. The reciprocal influence of the liver and blood stages of the malaria parasite's life cycle. *Int. J. Parasitol.* **2022**, 52(11), 711-15.
4. J.A. Garrido-Cardenas, L. González-Cerón, F. Manzano-Agugliaro, C. Mesa-Valle. Plasmodium genomics: an approach for learning about and ending human malaria. *Parasitol. Res.* **2019**, 118(1), 1-27.
5. P.A. Eckhoff. A malaria transmission-directed model of mosquito life cycle and ecology. *Malar. Jour.* **2011**, 10(1), 303.

6. M. Dhorda, C. Amaratunga, A.M. Dondorp. Artemisinin and multidrug-resistant Plasmodium falciparum – a threat for malaria control and elimination. *Curr. Opin. Infect. Dis.* **2021**, 34(5).
7. C. Rasmussen, P. Alonso, P. Ringwald. Current and emerging strategies to combat antimalarial resistance. *Expert. Rev. Anti. Infect. Ther.* **2022**, 20(3), 353-72.
8. B. Hanboonkunupakarn, N.J. White. Advances and roadblocks in the treatment of malaria. *Br. J. Clin. Pharmacol.* **2022**, 88(2), 374-82.
9. R.W. van der Pluijm, C. Amaratunga, M. Dhorda, A.M. Dondorp. Triple Artemisinin-Based Combination Therapies for Malaria – A New Paradigm? *Trends Parasitol.* **2021**, 37(1), 15-24.
10. I. Chen, M. S. Hsiang. Triple artemisinin-based combination therapies for malaria: a timely solution to counter antimalarial drug resistance. *Lancet Infect. Dis.* **2022**, 22(6), 751-53.
11. F.V. Rahmasari, P.B.S. Asih, F.K. Dewayanti et. al. Drug resistance of Plasmodium falciparum and Plasmodium vivax isolates in Indonesia. *Malar. Jour.* **2022**, 21(1), 354.
12. G. Quéléver, S. Bulet, C. Garino et. al. Simple Coupling Reaction between Amino Acids and Weakly Nucleophilic Heteroaromatic Amines. *J. Comb. Chem.* **2004**, 6(5), 695-98.
13. E.G. Tse, M. Korsik, M. H. Todd. The past, present and future of anti-malarial medicines. *Malar Jour.* **2019**, 18, 93
14. C. Upadhyay, N. Sharma, S. Kumar et. al. Synthesis of the new analogs of morpholine and their antiplasmodial evaluation against the human malaria parasite Plasmodium falciparum. *New J. Chem.* **2022**, 46(1), 250-62.
15. S. Kumar, C. Upadhyay, M. Bansal et. al. Experimental and Computational Studies of Microwave-Assisted, Facile Ring Opening of Epoxide with Less Reactive Aromatic Amines in Nitromethane. *ACS Omega* **2020**, 5(30), 18746-57.
16. W. Trager, J.B. Jensen. Human malaria parasites in continuous culture. *Science (N.Y.)* **1976**, 193(4254), 673-5.
17. G. Ciapetti, E. Cenni, L. Pratelli, A. Pizzoferrato. In vitro evaluation of cell/biomaterial interaction by MTT assay. *Biomaterials* **1993**, 14(5), 359-64.
18. P.P. Sharma, A. Sethi, B. Dwivedi, et al. Novel Inhibitors of malarial aspartyl proteases, plasmepsin II and IV: In silico design and validation studies. *Chem. Biol. Lett.* **2022**, 9 (1), 315.
19. A.K. Gautam, R. Boyina. Computational assisted designing, screening, and synthesis of novel Inhibitor of malarial aspartic proteases Plasmepsin I. *Chem. Biol. Lett.* **2022**, 9 (4), 364.
20. A. Daina, O. Michielin, V. Zoete. SwissADME: a free web tool to evaluate pharmacokinetics, drug-likeness and medicinal chemistry friendliness of small molecules. *Sci. Rep.* **2017**, 742717.
21. M. Gupta, H.J. Lee, C.J. Barden, D.F. Weaver. The Blood–Brain Barrier (BBB) Score. *J. Med. Chem.* **2019**, 62(21), 9824-36.